BIOLOGY OF REPRODUCTION (2016) **95**(5):107, 1–12
Published online before print 28 September 2016.
DOI 10.1095/biolreprod.116.142687

Rosiglitazone Improves Stallion Sperm Motility, ATP Content, and Mitochondrial Function[1]

Aleona Swegen,[2] Sarah Renay Lambourne, R. John Aitken,[3] and Zamira Gibb[3]

Priority Research Centre in Reproductive Science, School of Environmental and Life Sciences, University of Newcastle, Callaghan, New South Wales, Australia

ABSTRACT

Media used for equine sperm storage often contain relatively high concentrations of glucose, even though stallion spermatozoa preferentially utilize oxidative phosphorylation (OXPHOS) over glycolysis to generate ATP and support motility. Rosiglitazone is an antidiabetic compound that enhances metabolic flexibility and glucose utilization in various cell types, but its effects on sperm metabolism are unknown. This study investigated the effects of rosiglitazone on stallion sperm function in vitro, along with the possible role of AMP-activated protein kinase (AMPK) in mediating these effects. Spermatozoa were incubated with or without rosiglitazone, GW9662 (an antagonist of peroxisome proliferator-activating receptor-gamma), and compound C (CC; an AMPK inhibitor). Sperm motility, viability, reactive oxygen species production, mitochondrial membrane potential (mMP), ATP content, and glucose uptake capacity were measured. Samples incubated with rosiglitazone displayed significantly higher motility, percentage of cells with normal mMP, ATP content, and glucose uptake capacity, while sperm viability was unaffected. The percentage of spermatozoa positive for mitochondrial ROS was also significantly lower in rosiglitazone-treated samples. AMPK localized to the sperm midpiece, and its phosphorylation, was increased in rosiglitazone-treated spermatozoa. CC decreased sperm AMPK phosphorylation and reduced sperm motility, and successfully inhibited the effects of rosiglitazone. Inclusion of rosiglitazone in a room temperature sperm storage medium maintained sperm motility above 60% for 6 days, attaining significantly higher motility than sperm stored in control media. The ability of rosiglitazone to substantially alleviate the time-dependent deterioration of stallion spermatozoa by diverting metabolism away from OXPHOS and toward glycolysis has novel implications for the long-term, functional preservation of these cells.

AMPK, ATP, fertility, metabolism, mitochondria, PPAR, reactive oxygen species, rosiglitazone, spermatozoa, stallion, thiazolidinedione

INTRODUCTION

Understanding sperm energy metabolism is of utmost importance in improving the efficacy of equine assisted reproductive technologies. In particular, maximizing the chances of conception following artificial insemination necessitates the development of strategies to manage sperm metabolism so that these cells retain full functionality during their collection, in vitro storage, and subsequent insemination.

Spermatozoa of various mammalian species differ in the principal metabolic pathways that they engage to sustain sperm motility and sperm survival [1]. Stallion spermatozoa seem to rely predominantly on mitochondrial oxidative phosphorylation (OXPHOS), and less on glycolytic metabolism [2, 3]. OXPHOS has the advantages of rapidly producing high levels of ATP and facilitating higher sperm motility than that possible with glycolysis [4], although not without a price. Reactive oxygen species (ROS) are produced as a by-product of OXPHOS [5], with the mitochondria being the main site of ROS production by the spermatozoon [6]. In the short term, high ROS levels are indicative of healthy mitochondrial sperm metabolism and associated positively with equine field fertility [2]. However, spermatozoa that are continually exposed to high levels of ROS exhaust their antioxidant reserves and ultimately deteriorate as they engage the intrinsic apoptosis pathway to cell death [7, 8].

The term ''metabolic flexibility'' refers to the ability of cells to switch between different substrates for ATP generation, as exemplified by recent studies on the development of new therapeutic approaches to type 2 diabetes (reviewed in Ref. 9). In particular, the capacity of cells to switch to glucose utilization is important in times of cellular stress, when ATP demand is high, but oxygen availability low. This is rather pertinent to stallion spermatozoa, which (a) display a high demand for ATP and a poor capacity for glucose utilization, (b) predominantly use OXPHOS to meet their energy demands [2, 3], and (c) are often stored in low-oxygen and high-glucose environments in vitro. Viewed in this light, the preservation of stallion spermatozoa might benefit from interventions similar to those used to address diabetes that promote energy flux through the glycolytic pathway.

Glucose concentrations in semen extenders are often much higher than those found in oviductal fluids—for example, the commonly used Kenney extender contains 270 mM glucose, while mare oviductal fluid glucose is reported to be relatively low, at 110–370 μM [10]. Encouraging stallion spermatozoa to more effectively utilize this excess glucose as an energetic substrate would have several potential benefits: providing an additional fuel source for ATP production, facilitating metabolism under anaerobic conditions, and reducing mitochondrial load along with an associated decrease in mitochondrial ROS production [5].

Thiazolidinedione (TZD) compounds are a group of chemicals that have received much attention, due to their

[1]This study was supported by an Australian Research Council Linkage grant, the Hunter Valley Equine Research Centre, and Harness Racing Australia.
[2]Correspondence: Alena Swegen, Priority Research Centre in Reproductive Science, School of Environmental and Life Sciences, University of Newcastle, Callaghan, New South Wales 2308, Australia.
E-mail: aleona.swegen@uon.edu.au
[3]These authors are joint senior authors.

Received: 13 June 2016.
First decision: 28 July 2016.
Accepted: 19 September 2016.

eISSN: 1529-7268 http://www.biolreprod.org
ISSN: 0006-3363

ability to alleviate insulin resistance and improve systemic outcomes in obese and diabetic subjects [11–13]. More specifically, the TZD chemical, rosiglitazone, improves insulin sensitivity [14], and has been shown to restore metabolic flexibility [15] and increase cellular glucose uptake [16].

Since the 1990s, TZDs, including rosiglitazone, were thought to work predominantly via the activation of peroxisome proliferator-activating receptor gamma (PPARG) [17, 18], a nuclear receptor involved in a number of physiological functions, including glucose and lipid homeostasis [19, 20]. Being a nuclear receptor, PPARG exerts its downstream effects via genomic mechanisms, thus bearing minimal direct relevance to mature spermatozoa, given that these are transcriptionally silent cells and, therefore, not susceptible to altered gene expression [21]. However, more recent evidence suggests that at least some of the effects exerted by rosiglitazone are mediated via alternative, non-PPARG pathways [22]. This is an exciting development, because it raises the possibility that rosiglitazone, and perhaps other TZD chemicals, could have direct effects on glucose uptake and metabolic flexibility in spermatozoa.

Prominent among non-PPARG pathways postulated to mediate the effects of TZDs on metabolic flexibility is AMP-activated protein kinase (AMPK). Often referred to as a molecular ''fuel gauge,'' the activation of AMPK induces a metabolic shift from ATP-consuming to ATP-producing pathways in response to cellular ATP depletion, increasing glucose uptake and stimulating efficient glycolysis and beta oxidation of fatty acids [23–25]. The AMPK mechanism plays crucial roles in starvation, exercise, hibernation, and various forms of metabolic dysfunction, including obesity and diabetes [26–29]. Not only does AMPK provide the link between systemic metabolic pathologies and female infertility [30], its importance in sperm development and function is becoming increasingly apparent [31–35]. Stallion sperm appear to possess AMPK, but its involvement in sperm metabolism is, thus far, unclear [35]. If the AMPK system is indeed present and functional in stallion spermatozoa, it could be exploited to manipulate pathways of energy generation in these cells, such that AMPK-activating chemicals—such as rosiglitazone—might be valuable additions to sperm storage media.

Only one published study has attempted to examine the direct effects of rosiglitazone on sperm function; it was found that this compound increased glycolytic enzyme activity and reduced the triglyceride content of human spermatozoa [36]. This suggests that rosiglitazone does have the capacity to alter aspects of sperm metabolism, however, effects on other sperm parameters were not reported, and it is unclear whether sperm motility and survival were affected. In addition, the impact of rosiglitazone on spermatozoa from a species that does not primarily use glycolytic processes (such as the horse) remains unclear.

In the present study, we examined the hypothesis that rosiglitazone, an antidiabetic compound able to influence cellular metabolic flexibility via nongenomic means, will have a beneficial effect on the long-term functional preservation of equine spermatozoa in vitro. The results shed new light on the metabolic regulation of equine spermatozoa, and have significant implications for the future efficacy of the horse-breeding industry.

MATERIALS AND METHODS

Experimental Design

An initial rosiglitazone dose-response experiment was performed to determine whether rosiglitazone affects sperm motility, and to identify the lowest concentration at which there is a significant and consistent effect; this concentration was then selected to pursue further experiments dissecting the effects of rosiglitazone on motility, viability, mitochondrial superoxide production, mitochondrial membrane potential (mMP), ATP content, and glucose uptake capacity. In order to gain some insight into the mechanism potentially mediating the effects of rosiglitazone on spermatozoa, this set of experiments was also performed in the presence of two additional compounds: GW9662, an antagonist of PPARG [37], and Compound C (CC), an inhibitor of AMPK phosphorylation [38]. Following confirmation of the presence of AMPK and phospho-AMPK (i.e., activated AMPK) in stallion spermatozoa, the relationships between rosiglitazone, AMPK, and sperm function were further investigated by examining the effects of both rosiglitazone and the AMPK inhibitor on motility and AMPK phosphorylation, and the correlation between motility and AMPK status among high- and poor-quality samples. For all of the above experiments, samples were prepared by discontinuous gradient centrifugation to reduce contamination from other cell types and debris, and incubated at 37°C to reveal biologically relevant effects of the treatments examined. Finally, to assess the relevance of rosiglitazone to an applied sperm storage setting, an ambient temperature storage trial was carried out. Here, minimally processed sperm (not subjected to gradient centrifugation) were incubated at 22°C in an ambient temperature storage medium (equine Biggers, Whitten, and Whittingham [eBWW]) [39], with and without rosiglitazone, and motility recorded every 48 h for 6 days.

Materials

Unless otherwise stated, all chemicals were purchased from Sigma-Aldrich (St. Louis, MO). A modified BWW medium [40] containing 95 mM NaCl, 4.7 mM KCl, 1.7 mM $CaCl_2 \bullet 2H_2O$, 1.2 mM KH_2PO_4, 1.2 mM $MgSO_4 \bullet 7H_2O$, 25 mM $NaHCO_3$, 5.6 mM D-glucose, 275 μM sodium pyruvate, 3.7 μl/ml 60% sodium lactate syrup, 50 U/ml penicillin, 50 μg/ml streptomycin, 250 μg/ml gentamicin, 20 mM Hepes, and 0.1% (w/v) polyvinyl alcohol, with an osmolality of approx. 310 mOsm/kg, was utilized throughout this study. For room temperature sperm storage experiments, the medium was further modified by addition of 50 mM L-carnitine and 10 mM sodium pyruvate, as described previously [39]; this modified medium is termed eBWW throughout the study.

For discontinuous gradient centrifugation of spermatozoa, isotonic Percoll was prepared by supplementing 90 ml Percoll with 10 ml of 10× Ham F10 solution, 740 μl sodium lactate syrup, 3 mg sodium pyruvate, 210 mg sodium bicarbonate, and 100 mg polyvinyl alcohol. The 40% and 80% gradient layers were prepared by diluting this isotonic Percoll solution in BWW medium.

Antibodies used were as follows: AlexaFluor-488 goat anti-rabbit IgG from Molecular Probes (Eugene, OR); anti-rabbit IgG-horseradish peroxidase (HRP) from Calbiochem (La Jolla, CA); polyclonal anti-AMPKα1 + AMPKα2 antibody from Abcam (Cambridge, UK); rabbit polyclonal anti-AMPKα (phospho-Thr172) antibody for Western blotting and immunocytochemistry from GeneTex (San Antonio, TX); and rabbit monoclonal phospho-AMPKα for flow cytometry from Abcam.

Preparation of Spermatozoa

Institutional and New South Wales state government ethical approval was obtained for the use of animal material in this study (approval number A-2011-122). Equine spermatozoa were collected from three normozoospermic, mixed-breed pony stallions of proven fertility, aged between 6 and 12 yr, and held on institutionally approved premises, using a pony-sized Missouri artificial vagina (Minitube Australia, Ballarat, VIC, Australia). Sample collection occurred throughout the year, once or twice per week. Following collection, samples were immediately diluted with two parts warmed (37°C) Kenney extender [41] to one part semen in 50-ml Falcon tubes. Semen was kept at ambient temperature in a polystyrene box (20–25°C) and transported to the laboratory within 1 h of collection. The extended semen was subsequently fractionated on a Percoll gradient, using 40% and 80% Percoll fractions (GE Healthcare, Castle Hill, NSW, Australia) centrifuged for 30 min at $500 \times g$ (22°C). High-quality spermatozoa were recovered from the base of the 80% region of the gradient, centrifuged ($500 \times g$, 3 min), and subsequently resuspended in BWW medium, with or without respective treatments, at a concentration of 2×10^7 cells/ml. A NucleoCounter SP-100 (ChemoMetec, Allerod, Denmark) was used to determine sperm concentration. With the exception of the room temperature sperm storage trial, experiments were performed by incubating sperm treatments at a volume of 1 ml, in 1.5-ml tubes, at 37°C. This temperature was used in order to facilitate observation of biologically relevant changes to sperm physiology, and to determine whether treatments are potentially able to alleviate the deterioration in sperm functionality seen under these conditions. A room temperature storage trial was also performed to determine the relevance of rosiglitazone-mediated changes to an applied sperm storage setting; spermatozoa were stored at 22°C in eBWW with and without rosiglitazone for 6 days,

and sampled every 48 h for motility analysis. For this experiment, samples were not subjected to gradient centrifugation, but were centrifuged (15 min at 500 × *g*, 22°C) to remove Kenney extender used during transportation of samples to the laboratory, prior to incubation in respective treatments.

For analysis of the relationship between motility and AMPK phosphorylation, lower-quality spermatozoa were also recovered from the 40%–80% Percoll interface (and subsequently processed as above) in order to provide a wider spectrum of sperm quality in the samples assessed. Each experiment was performed on at least three ejaculates per stallion (n = 9).

Motility Analysis

Sperm motility was objectively determined using computer-assisted sperm analysis (IVOS; Hamilton Thorne, Danvers, MA) using the following settings: negative phase-contrast optics, recording rate of 60 frames/sec, minimum contrast of 70, minimum cell size of 4 pixels, low-size gate of 0.17, high-size gate of 2.9, low-intensity gate of 0.6, high-intensity gate of 1.74, nonmotile head size of 10 pixels, nonmotile head intensity of 135, progressive average path velocity (VAP) threshold of 50 μm/sec, slow (static) cells VAP threshold of 20 μm/sec, slow (static) cells straight line velocity (VSL) threshold of 0 μm/sec, and threshold straightness (STR; i.e., VSL/VAP) of 75%. Cells exhibiting a VAP of ≥50 μm/sec and a STR of ≥75 were considered progressive. Cells with a VAP greater than that of the mean VAP of progressive cells were considered rapid. A minimum of 200 total spermatozoa and a minimum of 5 fields were assessed using 20 μm Leja standard count slides (Gytech, Armadale North, VIC, Australia) and a stage temperature of 37°C.

Flow Cytometry Measurements

Flow cytometry was performed using a FACSCalibur flow cytometer (Becton Dickinson, Franklin Lakes, NJ) with a 488-nm argon ion laser. Emission measurements were made using 530/30-nm band-pass (green/FL-1), 585/42-nm band-pass (red/FL-2), and >670-nm long-pass (far red/FL-4) filters. Forward-scatter and side-scatter plots were used to gate sperm cells only and exclude contaminating cells and debris. All data were acquired and analyzed using CellQuest Pro software (Becton Dickinson) with a total of 5000 events collected per sample.

Mitochondrial ROS generation was measured in live cells by incubating spermatozoa with 2 μM MitoSOX Red (MSR; Molecular Probes, Australia) and 5 nM Sytox Green vitality stain (Molecular Probes, Australia) for 15 min at 37°C, followed by a single centrifugation and wash in BWW. Samples were assessed via flow cytometry and the percentage of live cells positive for MSR recorded. A sperm sample treated with 50 μM arachidonic acid served as a positive MSR control, and a boiled sperm sample was used as a positive Sytox Green control [42].

Mitochondrial membrane potential was assessed by incubating spermatozoa with 2 μM JC-1 (Molecular Probes, Australia) at ambient temperature for 30 min using 10 μM carbonyl cyanide *m*-chlorophenylhydrazone-treated cells as a negative control.

For assessment of AMPK phosphorylation by flow cytometry, spermatozoa were first exposed to Live/Dead Fixable Far Red Dead Cell stain (Molecular Probes, Australia), fixed in 2% paraformaldehyde, and stored at 4°C until further analysis. For Live/Dead staining, spermatozoa were incubated at 37°C for 20 min with reconstituted stain at a concentration of 1 μl/ml, then washed in BWW by centrifugation at 500 × *g* (3 min at 22°C), fixed in 2% paraformaldehyde for 10 min, washed in PBS, and stored in 0.1 M glycine in PBS (4°C) for up to 1 wk. On the day of assessment, cells were permeabilized in a solution of PBS containing 0.1% Triton X-100 and 3.4 mM sodium citrate for 5 min at 4°C, pelleted via centrifugation, blocked in 10% goat serum in 0.1 M glycine/PBS for 1 h at 22°C, washed in PBS, and incubated with anti-phospho-AMPK antibody (1:200 in 0.1 M glycine/PBS) for 30 min at 37°C. Cells were washed and resuspended in secondary antibody (AlexaFluor-488 goat anti-rabbit IgG) for 15 min at 37°C (1:100), centrifuged again, washed twice with PBS, and resuspended in 300 μl of PBS for analysis by flow cytometry. Flow cytometry gates were set using a boiled sperm sample for Live/Dead-positive control, and secondary-only-stained sample for negative AMPK phosphorylation control. Geometric mean of fluorescence intensity (GMFI) of AlexaFluor-488 (green fluorescence, FL-1) was taken to indicate extent of AMPK phosphorylation, measured after dead cells (far-red fluorescence positive, FL-4) were gated out of the analysis plot.

For glucose uptake measurement, Percoll-processed spermatozoa were washed once in glucose-free BWW and incubated (200 μl at 2×10^7 million/ml) with or without rosiglitazone and GW9662, in glucose-free BWW medium containing 100 μg/ml fluorescent D-glucose analog, 2-(N-[7-nitrobenz-2-oxa-1,3-diazol-4-yl] amino)-2-deoxy-D-glucose (2-NBDG; Cayman Chemical Company, Ann Arbor, MI). Samples were incubated overnight at 37°C as for other experiments involving rosiglitazone. The following day, samples were centrifuged at 500 × *g* (3 min) and resuspended with Live/Dead Fixable Far Red Dead Cell stain (1 μl/ml in glucose-free BWW) for 20 min at 37°C, followed by a single wash in glucose-free BWW and analysis by flow cytometry. The GMFI of 2-NBDG (green fluorescence, FL-1) was taken to indicate the cellular capacity to take up glucose measured after dead (far-red fluorescence positive, FL-4) cells were gated out of the analysis plot. As specified above, flow cytometry gates were set using a boiled sperm sample for Live/Dead-positive control.

ATP Measurements

ATP levels were measured using an ATP bioluminescence assay kit (Sigma-Aldrich, Australia) following the manufacturer's instructions. This assay relies on the conversion of ATP and D-luciferin into oxyluciferin, AMP, and CO_2 accompanied by production of light; this emission of light is proportional to the amount of ATP present, and is the output measured by the luminescence system. Briefly, 1-ml aliquots containing 20×10^6 spermatozoa were centrifuged down to a pellet and resuspended in boiling ultrapure water to extract ATP. Samples were placed on ice and sperm concentration counts performed for each sample in order to accurately normalize ATP levels to sperm number. Samples were centrifuged at 20 000 × *g* for 10 min at 4°C. The supernatant was retained and utilized for the assay. The ATP standard solution supplied with the kit was serially diluted to obtain concentrations of 0.3 nM to 3 μM. The luciferin-luciferase reagent (100 μl) was equilibrated for 3 min at 22°C in a Berthold AutoLumat luminometer LB-953 (Berthold, Bad Wildbad, Germany). Samples and standards (100 μl) were then added, and the resulting chemiluminescence was monitored for a further 5 min, and the results expressed as integrated counts. Media blanks were run in order to ensure that the signals recorded were not due to the spontaneous activation of the probe.

Immunocytochemistry

To ascertain the localization of AMPK in spermatozoa, samples of approximately 2×10^6 cells (100 μl) were first stained with Live/Dead Fixable Far Red Dead Cell stain by incubation with the Live/Dead stain (1 μl/ml) for 30 min at 37°C, followed by a single wash in BWW. Cells were then fixed in 2% paraformaldehyde (4°C for 10 min), washed in PBS, permeabilized with 0.1% Triton X-100 and 3.4 mM sodium citrate in PBS for 5 min at 4°C, pelleted via centrifugation, blocked in 10% goat serum in 0.1 M glycine/PBS for 1 h at 22°C, washed in PBS, and incubated with the respective antibodies (anti-phospho-AMPK antibody at 1:200 or anti-AMPK at 1:100 in 0.1 M glycine/PBS) for 1 h at 37°C. Cells were washed and resuspended with secondary antibody (AlexaFluor-488 goat anti-rabbit IgG) for 1 h at 37°C (1:100 in PBS), centrifuged again, washed twice with PBS, resuspended, and mounted on slides. Prepared samples were visualized and imaged using a fluorescence microscope (Axio Imager A1; Carl Zeiss MicroImaging GmbH, Jena, Germany).

SDS-PAGE/Western Blot

Sperm samples (approximately 2×10^7 cells) were lysed by boiling for 10 min in SDS extraction buffer (100 mM Tris, 146 mM sucrose, 1% [w/v] SDS). Samples were centrifuged and supernatant collected. Protein content was quantified using a DC kit (Bio-Rad, Castle Hill, NSW, Australia) per the manufacturer's instructions. Approximately 10 μg of protein from spermatozoa was boiled in SDS-PAGE sample buffer (SDS extraction buffer as described above, supplemented with 2% β-mercaptoethanol and bromophenol blue) for 5 min and resolved on 4%–20% polyacrylamide gels (NuSep, Sydney, NSW, Australia). Proteins were then transferred to nitrocellulose membranes under a constant current of 350 mA for 1 h. Nitrocellulose membranes were blocked for 1 h in 3% bovine serum albumin (BSA) in Tris-buffered saline (TBS; 100 mM Tris-HCl, pH 7.6, and 150 mM NaCl) supplemented with 0.1% Tween 20 (TBST). Membranes were rinsed in TBST and probed overnight at 4°C with anti-AMPK or anti-phospho-AMPK antibody at a 1:500 dilution in TBST with 1% BSA, rinsed with TBST, and then probed for 1 h with a 1:3000 dilution of HRP-conjugated secondary antibody (in TBST with 1% BSA) at room temperature. After a further three washes in TBST, cross-reactive proteins were visualized using an enhanced chemiluminescence kit (GE Healthcare, Piscataway, NJ) according to the manufacturer's instructions. The phospho-AMPK blots were stripped and reprobed with anti-tubulin antibody as a loading control. Band intensity was quantified using MultiGauge software (Fujifilm, Tokyo, Japan), with results reported as arbitrary units (AU) minus background (BG) of each band, expressed as a ratio to tubulin loading control, i.e. AU-BG(sample):AU-BG(tubulin).

Statistical Analysis

Results are presented as means ± SEM. Measurements of fluorescence intensity are expressed as percentage of fluorescence intensity of the untreated control sample within that replicate. Significance of difference between treatments was set at $P < 0.05$ and was calculated by Wilcoxon nonparametric test comparing treatments against the untreated control. Spearman rank correlation analysis was used to determine correlation between sperm parameters. Excel for Mac 2011 (Microsoft, Bellevue, WA) and JMP v11.2 (SAS Institute, Cary, NC) were used for statistical analyses.

RESULTS

Effects of Rosiglitazone Treatment on Stallion Spermatozoa

Spermatozoa treated with rosiglitazone exhibited significantly higher total and rapid motility than untreated samples by 24 h of incubation at 37°C (Fig. 1B). Since no significant differences in motility were observed at 1 h of incubation (Fig. 1A), subsequent sperm analyses were carried out at the 24-h time point, as we were interested in the changes to sperm physiology temporally associated with maximal effects of rosiglitazone. In order to ascertain whether the motility-enhancing effects of rosiglitazone were mediated via the PPARG pathway, or via AMPK phosphorylation, respectively, GW9662 (a PPARG antagonist) and CC (an AMPK phosphorylation inhibitor) were added to rosiglitazone incubations. While GW9662 had no significant impact on the response to rosiglitazone, CC completely suppressed motility in the absence of any impact on sperm viability (Fig. 2, A–C). Similarly, the ability of rosiglitazone to inhibit mitochondrial ROS generation while increasing mMP was unaffected by GW9662, but completely reversed by CC (Fig. 2, D and E). In concert with the stimulation of mitochondrial activity and motility, the ATP content of stallion spermatozoa increased dramatically in the presence of rosiglitazone; the increase remained unimpeded by GW9662, but was inhibited by CC (Fig. 2F). The sperm capacity for glucose uptake also showed a dose-dependent increase in response to rosiglitazone that was not influenced by the concomitant presence of GW9662, but was significantly countered by the presence of CC (Fig. 2G). Values for sperm motility, viability, mitochondrial ROS, mMP, ATP, and glucose uptake measurements shown in Figure 2 are presented in Table 1.

Sperm AMPK and AMPK Phosphorylation in the Presence of Rosiglitazone

Immunocytochemistry indicated that both total AMPK (α1 and α2 subunit) and AMPK phosphorylated at Threonine-172 are present in stallion spermatozoa (Fig. 3, A and B) and are distinctly predominant in the midpiece. The presence of total AMPK in stallion spermatozoa was further confirmed by Western blotting of sperm SDS extracts with AMPK α1/α2 antibody; a representative blot is shown in Figure 4A. The bands obtained consistently matched the molecular weights of AMPK dimers, and of multimeric complexes reported in previous studies [43] that employed small angle x-ray scattering and electron microscopy to dissect the dimerization behavior and structural properties of AMPK. In Figure 4A, bands at 215 and ~140 kDa represent heterotrimers (αβγ), as described by Riek et al. [43]. Bands at 100 and 120 kDa may represent αγ complexes, and correspond with the appropriate predicted molecular weights of subunits documented for equine AMPK (α1 at 59.24 kDa, α2 at 59.02 kDa, γ1 at 37.36 kDa, and γ2 at 62.47 kDa). The band at 60 kDa corresponds with molecular weights of single AMPK α1 and α2 subunits, while

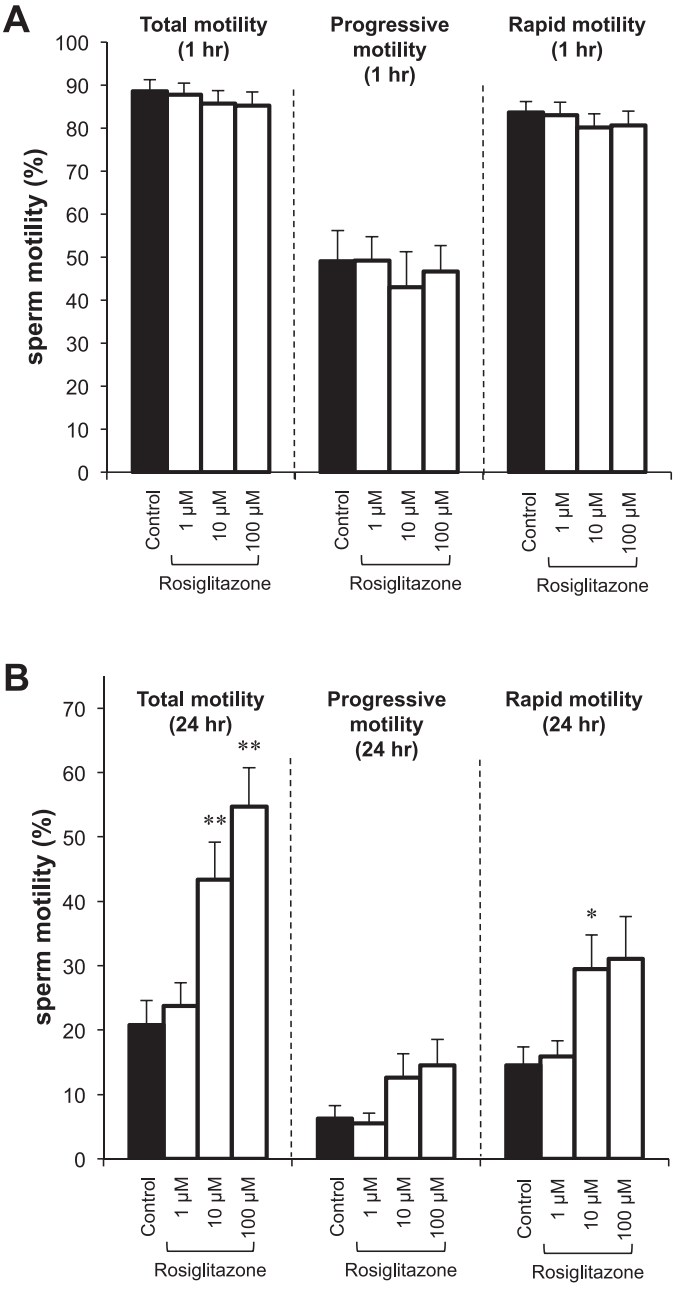

FIG. 1. Rosiglitazone improves motility in stallion spermatozoa. **A** and **B**) Percoll-processed spermatozoa were incubated with 0–1, 10, and 100 μM rosiglitazone in BWW medium at 37°C (n = 9); motility analyses were performed using computer-assisted sperm analysis (CASA) at 1 and 24 h of incubation. Bar graphs represent mean values ± SEM; significant difference from the control determined by nonparametric Wilcoxon test, indicated by $*P < 0.05$, $**P < 0.01$.

a ~83-kDa band is likely to be the same partially dissociated complex identified by Riek et al. [43].

Flow cytometric analysis of anti-phospho-AMPK fluorescence intensity indicated that phosphorylation of AMPK is increased in samples of stallion spermatozoa preincubated for 24 h with 10 μM and 100 μM rosiglitazone (Fig. 4B). This result was supported by Western blot data (Fig. 4A). Furthermore, a positive correlation between AMPK phosphorylation and total motility in untreated spermatozoa suggests that sperm motility may be affected by AMPK phosphorylation status (Fig. 4C); correlation analysis of AMPK phosphorylation

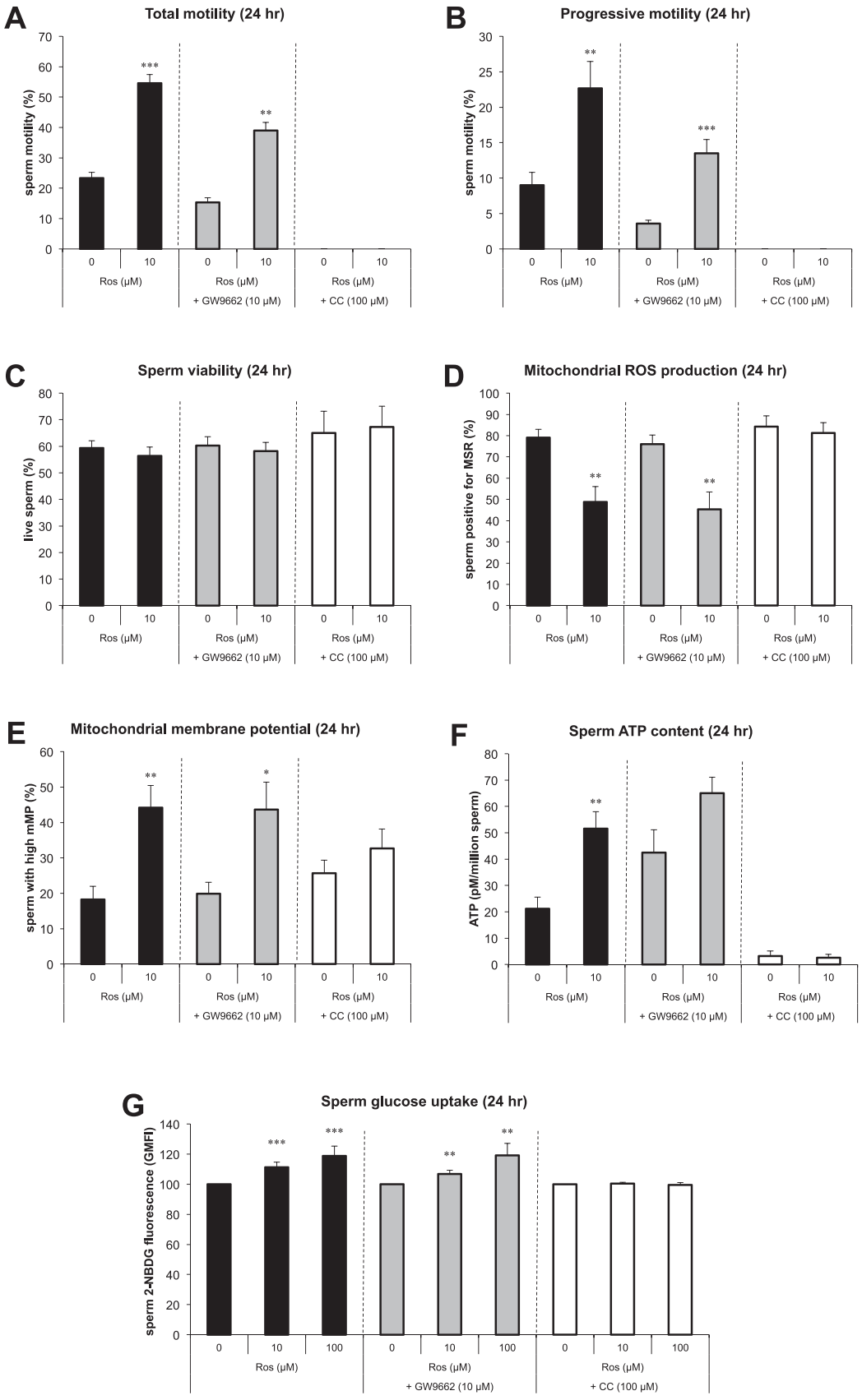

FIG. 2. Effects of rosiglitazone treatment, a PPARG antagonist and an AMPK inhibitor, on stallion sperm motility, viability, mitochondrial function, ATP content, and glucose uptake capacity. Percoll-processed spermatozoa were incubated for 24 h at 37°C with or without rosiglitazone, in BWW, BWW + 10 μM PPARG antagonist GW9662, or BWW + 100 μM AMPK inhibitor, CC. **A** and **B**) Motility analyses were performed using CASA (n = 12). **C**) Sperm viability was determined using Live/Dead Fixable Far Red stain and flow cytometry (n = 11). **D**) Mitochondrial superoxide generation was assessed in live cells using MSR, counterstained with Sytox Green vitality stain. Samples were assessed via flow cytometry and the percentage of live cells positive for MSR

TABLE 1. Effects of rosiglitazone treatment, a PPARG antagonist (10 μM GW9662) and an AMPK inhibitor (100 μM CC), on stallion sperm motility, viability, mitochondrial function, ATP content, and glucose uptake capacity.[a]

Treatment	Total motility (24 h; % motile sperm)[b]	Progressive motility (24 h; % motile sperm)[b]	Sperm viability (24 h; % live sperm)[b]	Mitochondrial ROS: sperm positive for MSR (24 h; %)[b]	Mitochondrial membrane potential: sperm with high mMP (24 h; %)[b]	Sperm ATP content (24 h; pM/million sperm)[b]	Glucose uptake: 2-NBDG fluorescence (24 h; GMFI; % of control)[b]
Ros							
0	23.3 ± 1.9	9.0 ± 1.8	59.3 ± 2.8	79.1 ± 3.9	18.3 ± 3.8	21.2 ± 4.4	100.0 ± 0.0
10 μM	54.6 ± 2.9***	22.7 ± 3.8**	56.4 ± 3.3	48.8 ± 7.3**	44.2 ± 6.2**	51.6 ± 6.4**	111.3 ± 3.5***
100 μM							118.8 ± 6.6***
Ros + GW9662							
0	15.3 ± 1.5	3.6 ± 0.5	60.3 ± 3.3	76.0 ± 4.3	19.9 ± 3.2	42.5 ± 8.7	100.0 ± 0.0
10 μM	39.0 ± 2.7**	13.5 ± 2.0***	58.2 ± 3.3	45.3 ± 8.2**	43.6 ± 7.7*	65.0 ± 6.1	106.8 ± 2.5**
100 μM							119.2 ± 8.1**
Ros + CC							
0	0.0 ± 0.0	0.0 ± 0.0	65.0 ± 8.2	84.2 ± 5.2	25.7 ± 3.7	3.2 ± 2.0	100.0 ± 0.0
10 μM	0.0 ± 0.0	0.0 ± 0.0	67.3 ± 7.7	81.3 ± 4.9	32.7 ± 5.4	2.6 ± 1.3	100.5 ± 0.8
100 μM							99.6 ± 1.5

[a] 2-NBDG, 2-deoxy-2-[(7-nitro-2,1,3-benzoxadiazol-4-yl)amino]-D-glucose; mMP, mitochondrial membrane potential; MSR, MitoSOX Red; ROS, reactive oxygen species; Ros, rosiglitazone.
[b] Values presented are mean ± SEM. Asterisks represent significant difference from the BWW control, GW9662-only control, or CC-only control: *$P < 0.05$, **$P < 0.01$, ***$P < 0.001$, determined by nonparametric Wilcoxon test.

versus viability and motility versus viability in the same sample cohort did not yield statistically significant correlations (data not shown).

Effects of an AMPK Inhibitor, CC, on Stallion Spermatozoa

Incubation of spermatozoa with CC, an inhibitor of AMPK phosphorylation, induced a clear, dose-dependent decrease in sperm motility (Fig. 5A), with no major effect on sperm viability (Fig. 5B). Phospho-AMPK fluorescence intensity decreased in a dose-dependent fashion, with 50- and 100-μM treatments resulting in phospho-AMPK fluorescence significantly lower than in control samples (Fig. 5C).

Inclusion of Rosiglitazone in a Room Temperature Sperm Storage Medium

Initial experiments examining concentrations of 10–100 μM indicated 50 μM as an optimal concentration for inclusion of rosiglitazone in a room temperature sperm storage medium containing L-carnitine and sodium pyruvate (eBWW). Medium containing rosiglitazone prevented decline of sperm motility for 6 days of incubation at 22°C, with significantly higher motility than eBWW alone at 144 h (Fig. 6).

DISCUSSION

This study aimed to examine the effect of rosiglitazone on stallion sperm function in vitro. Its conception stemmed from the postulate that rosiglitazone, as an antidiabetic agent with nongenomic activity, would enhance the metabolic flexibility of spermatozoa. We proposed that this would allow spermatozoa to take up and metabolize glucose with greater efficiency, and thus provide an additional source of fuel for the production of ATP to support motility, along with the added benefits of low oxygen demand and reduced ROS production. We found that rosiglitazone treatment of stallion spermatozoa in biologically relevant conditions (37°C incubation) did indeed result in significantly higher motility and ATP levels compared to untreated samples (Figs. 1B and Fig. 2, A and F, respectively). Rosiglitazone also exerted a protective effect on sperm mitochondria, as indicated by the proportion of sperm cells with high mMP (Fig. 2D). This was accompanied by much lower production of superoxide (Fig. 2D), suggesting either a more efficient mitochondrial metabolism, or a shift away from mitochondrial metabolism toward glycolytic pathways. Higher sperm ATP content, alongside increased glucose uptake induced by rosiglitazone, suggests the latter.

Secondarily, this study aimed to probe the possible mechanisms that might sustain the positive effects of rosiglitazone on stallion spermatozoa. It has been previously suggested that rosiglitazone exerts its effects on spermatozoa via activation of PPARG [36], yet, while stallion spermatozoa do appear to express PPARG [44], there is little evidence to support its involvement in rosiglitazone's effects on spermatozoa [36]. Furthermore, PPARG is a nuclear receptor the action of which is via genomic means: the binding of a ligand induces a process of gene transcription that leads to physiological changes in the cell [19]. Meanwhile, spermatozoa are terminally differentiated cells, and do not sustain active transcription of genes in their postejaculation form [21]. While it is not uncommon for nuclear receptors to have additional functions of a nongenomic nature, it is unclear whether PPARG is capable of such activity. Therefore, PPARG activation seems a very unlikely explanation for the effects

recorded (n = 11). **E**) Mitochondrial membrane potential was assessed by incubating spermatozoa with JC-1. Percentages of cells with high-red JC-1 fluorescence (high mMP) were recorded by flow cytometry (n = 12). **F**) Sperm ATP content was measured using a Sigma-Aldrich ATP bioluminescence assay kit and luminometry following ATP extraction from sperm pellets using boiling ultrapure water. Sperm counts were performed prior to ATP extraction and used to calculate ATP concentration in pM per million spermatozoa (n = 6). **G**) Sperm capacity for glucose uptake was measured using green fluorescence D-glucose analog, 2-NBDG, in glucose-free medium. Results are presented as GMFI of live cells, as measured by flow cytometry, expressed as percentage of respective untreated control sample intensity (n = 14). Bar graphs represent mean values ± SEM. Asterisks represent significant difference from the BWW control, GW9662-only control, or CC-only control. *$P < 0.05$, **$P < 0.01$, ***$P < 0.001$, determined by nonparametric Wilcoxon test. GW, GW9662.

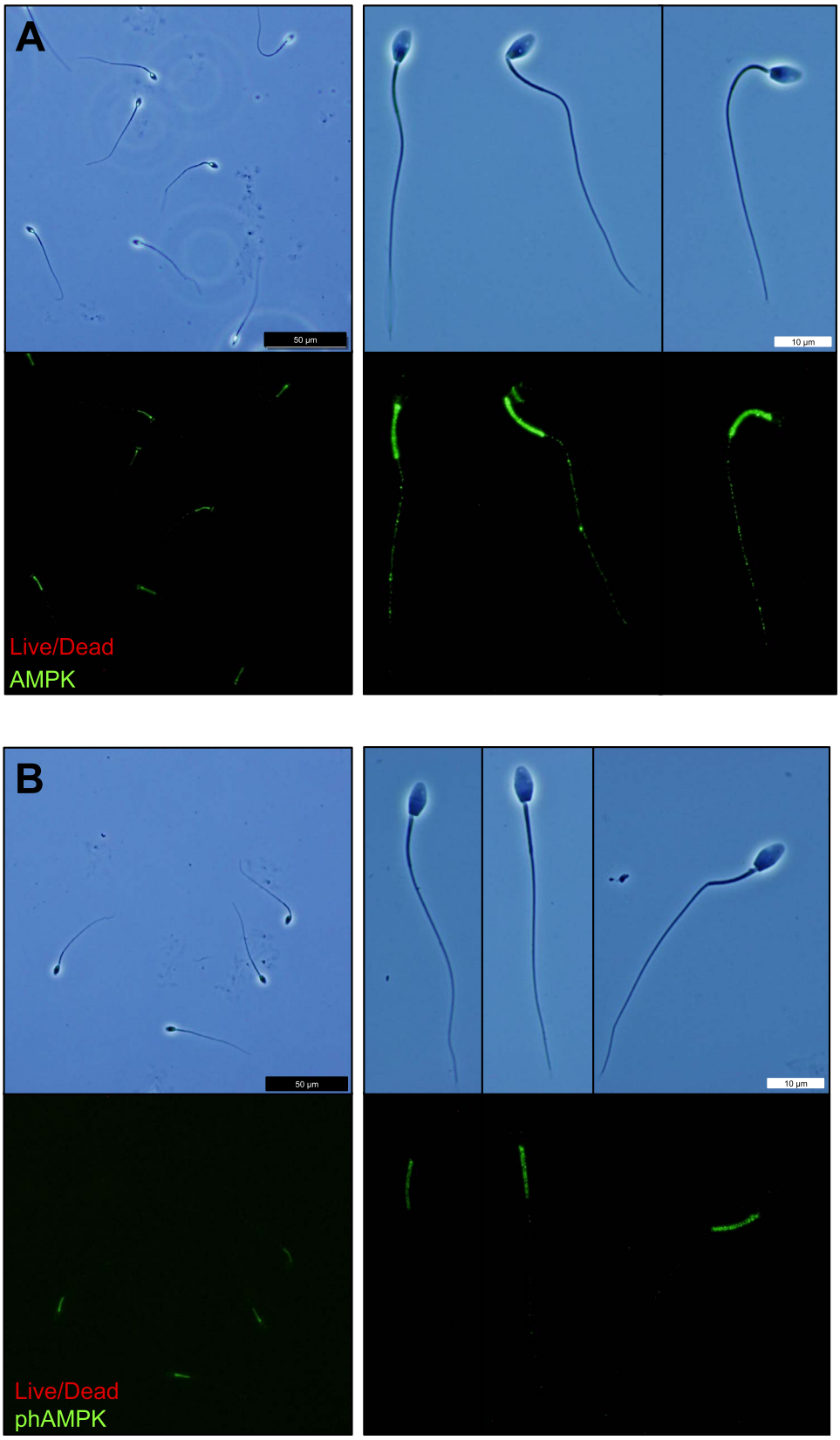

FIG. 3. AMPK localization in stallion spermatozoa. Localization of total AMPKα and phosphorylated AMPK was determined using rabbit polyclonal anti-AMPK (α1 + α2) antibody and rabbit polyclonal anti-phospho (Thr172)-AMPK, respectively, together with AlexaFluor-488 secondary antibody. Live/Dead Fixable Far Red stain was used to distinguish live and dead cells; dead sperm display red fluorescence. Spermatozoa were imaged at 200× (left-hand panels) and 1000× (right-hand panels) magnification. **A**) AMPK appears predominantly in the midpiece with minor punctate staining along the flagellum. All sperm consistently display total AMPK fluorescence. **B**) Phospho (Thr172)-AMPK (phAMPK) is prominent only in the midpiece of stallion spermatozoa. Intensity of phAMPK fluorescence varies between cells.

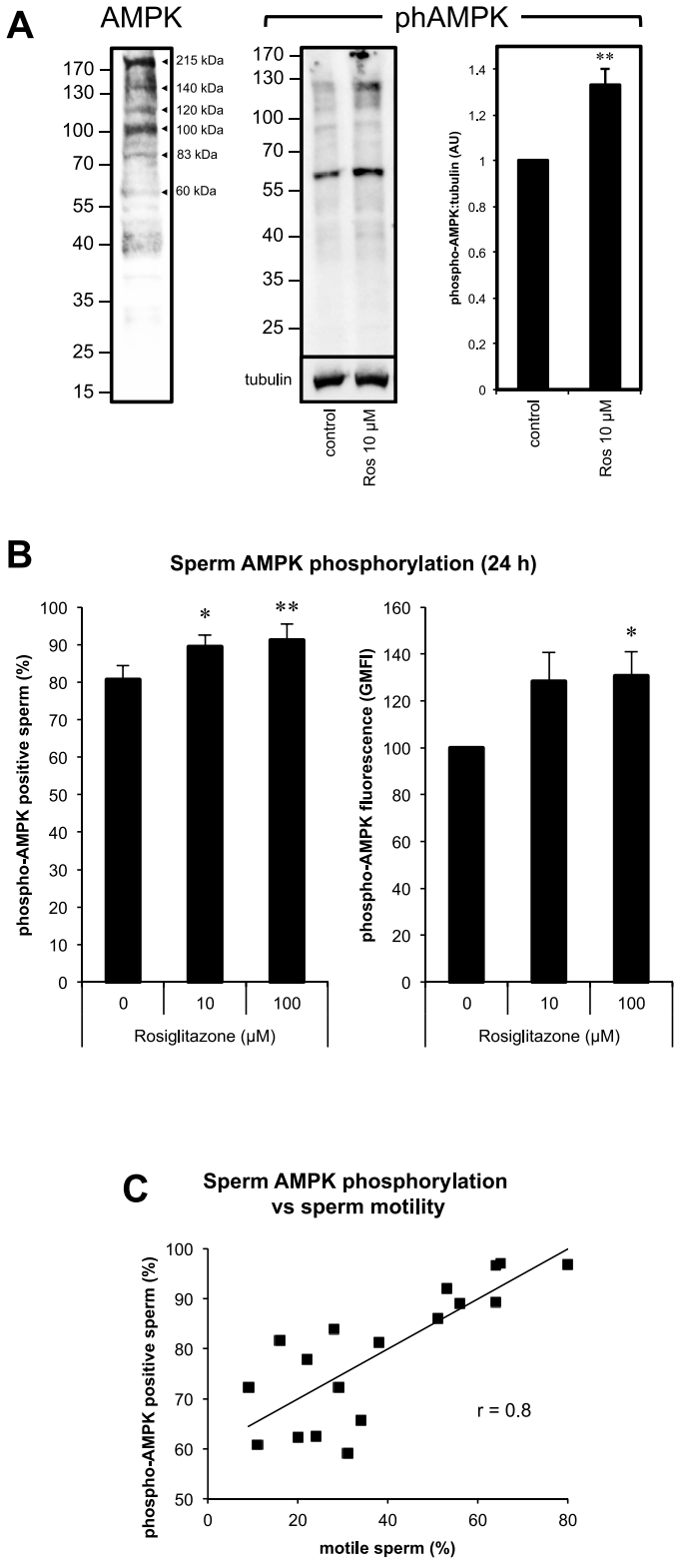

FIG. 4. AMPK phosphorylation in stallion spermatozoa treated with rosiglitazone. **A**) Western blot with total AMPKα1/α2 antibody confirms AMPK in stallion spermatozoa is present in multiple complexes, thee molecular weights of which correspond with AMPK subunit- and heterotrimer-monomers and dimers. Blotting with anti-phospho (Thr172)-AMPK antibody displays an increase in 59-kDa band intensity for rosiglitazone-treated samples, normalized against tubulin loading control (n = 8; representative image shown). **B**) Percoll-processed spermatozoa were incubated for 24 h at 37°C in BWW with or without rosiglitazone. AMPK phosphorylation was compared between treatments by labelling with anti-phospho-AMPK antibody and AlexaFluor-488 secondary, counterstained with Live/Dead Fixable Far Red vitality stain. Percentage of phospho-AMPK-positive spermatozoa, as well as the geometric mean intensity of phospho-AMPK fluorescence, were measured by flow cytometry (n = 13). Only live cells were included in the analysis. **C**) Spermatozoa were recovered from the low- and high-quality fractions of a Percoll gradient in order to compare AMPK phosphorylation and total sperm motility in a range of samples (n = 18). Spearman rank correlation analysis of CASA and anti-phospho-AMPK flow cytometry data revealed a positive correlation between total sperm motility and AMPK phosphorylation in untreated samples: $r = 0.8$ ($P < 0.001$). Bar graphs represent mean values ± SEM. Asterisks represent significant difference from the control. $^{*}P < 0.05$, $^{**}P < 0.01$, determined by nonparametric Wilcoxon test.

of rosiglitazone on spermatozoa. This is largely in accordance with our own results, in which the irreversible PPARG antagonist, GW9662, failed to inhibit the effects of rosiglitazone on spermatozoa (Fig. 2, A–G). An exception to this was sperm motility, where a partial inhibition was seen (Fig. 2, A and B); however the negative effects on motility of GW9662 alone somewhat confound these results and raise doubts as to the specificity of this chemical. Indeed, there is evidence in the literature of GW9662 having non-PPARG effects in other cell types, specifically by interference with tubulin [45]. Notably, these effects appear to take place at a posttranscriptional level, and, given that tubulin is integral to maintaining sperm flagellar structure and motility [46], provide a fitting explanation for the decrease in sperm motility seen with GW9662 in our study. How GW9662 alone might increase sperm ATP content (Fig. 2F) is unclear, but may be the consequence of reduced ATP consumption by spermatozoa with decreased motility.

Having established PPARG activation as an unlikely mechanism for the effects of rosiglitazone, we shifted our attention to alternative pathways that do not involve gene transcription, but might explain rosiglitazone's ability to improve cellular metabolic flexibility. One of the recently reported nongenomic mechanisms of TZD action is the activation of AMPK, an important regulator of cellular energy balance [23–25]. Phosphorylation of AMPK is usually induced by an increased AMP:ATP ratio, encountered when ATP is depleted during metabolic stress, starvation, hibernation, and exercise, or by pharmacological agents. Phosphorylation activates AMPK, initiating a cascade of downstream intracellular signals that culminate in increased catabolism and glucose uptake, and restoration of ATP levels. It appears that the AMPK system is functional in every cell type investigated thus far, with early evidence of its activity in spermatozoa of boar [47], stallion [35], and chicken [34]. Rosiglitazone has been shown to activate AMPK in multiple cells types: for example, a dramatic increase in phosphorylation was seen in muscle cells [25], while AMPK activation by rosiglitazone improved survival in beta cells of the pancreas [23]. It is this activation of AMPK, rather than PPARG, that is increasingly deemed responsible for the insulin-sensitizing properties of rosiglitazone [48].

Given the role of AMPK in stimulating ATP production and glucose uptake, alongside rosiglitazone's reported ability to activate this important metabolic regulator, the AMPK signaling pathway presented an appealing explanation for rosiglitazone's effects on spermatozoa during this study. We confirmed the presence of AMPK and phospho-AMPK in the midpiece of stallion spermatozoa (Fig. 3), an appropriate localization for a sensor of ATP depletion, given that the mitochondria residing in this region are the main site of ATP production. The AMPK inhibitor, CC, successfully abrogated most of the effects of rosiglitazone on spermatozoa, lending

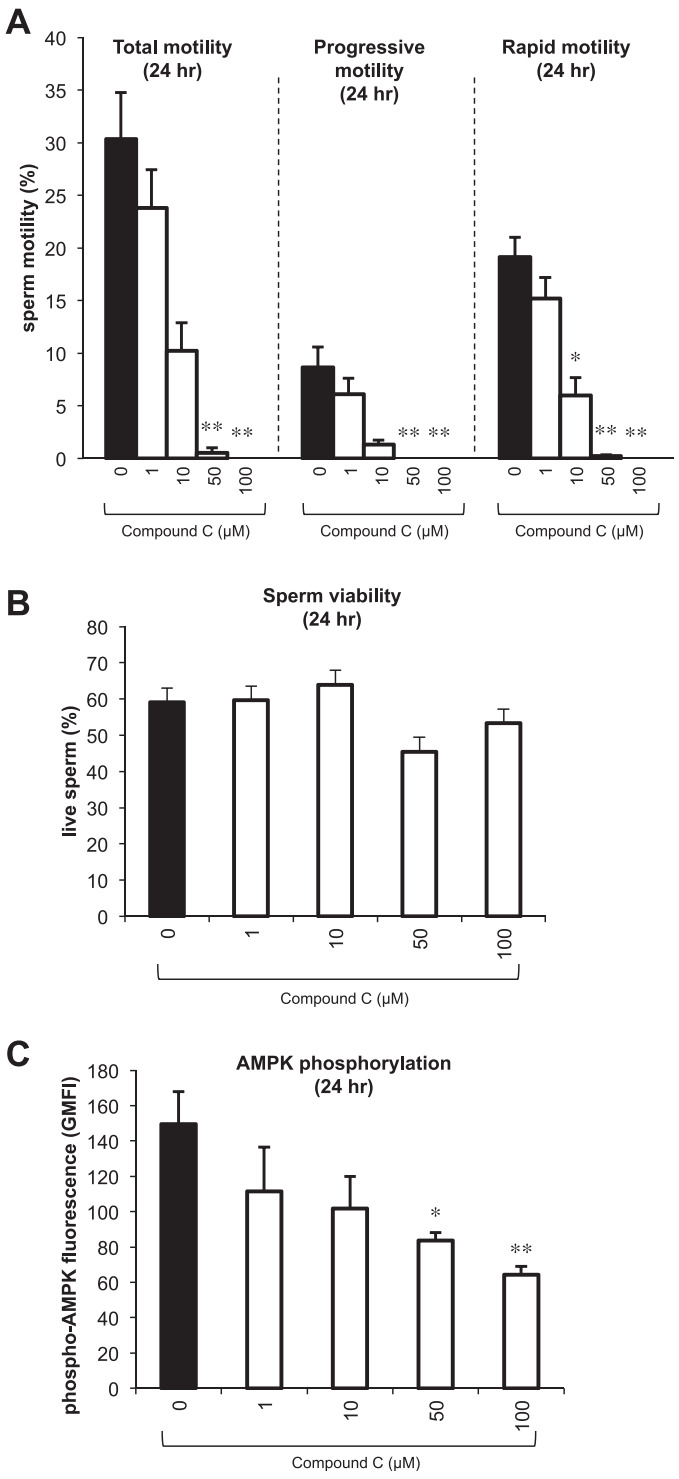

FIG. 5. Effects of a pharmacological AMPK phosphorylation inhibitor on stallion sperm motility, viability, and AMPK phosphorylation. Percoll-processed spermatozoa were incubated for 24 h at 37°C in BWW with or without CC. **A**) Motility analyses were performed using CASA (n = 9). **B**) Sperm viability was determined using Live/Dead Fixable Far Red stain and flow cytometry (n = 6). **C**) AMPK phosphorylation was assessed using anti-phospho-AMPK antibody and AlexaFluor-488 secondary. The GMFI of the live cell population (determined using Live/Dead Fixable Far Red stain) was measured using flow cytometry (n = 6). Bar graphs represent mean values ± SEM. Asterisks represent significant difference from the control, determined by nonparametric Wilcoxon test. $^{*}P < 0.05$, $^{**}P < 0.01$.

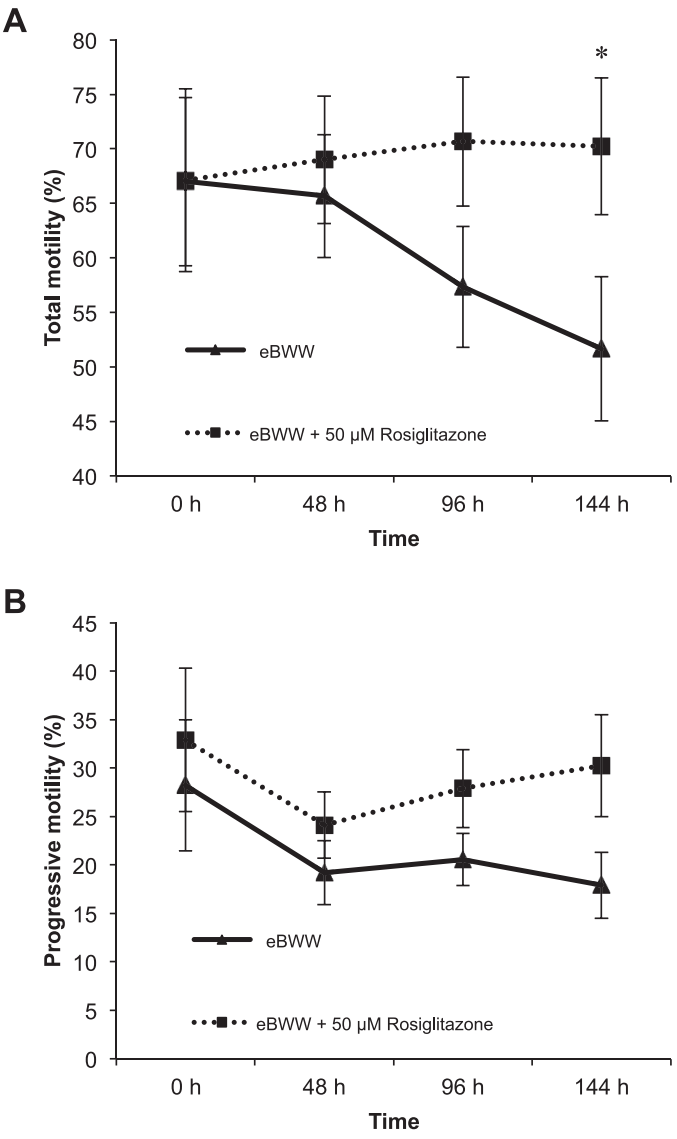

FIG. 6. Inclusion of rosliglitazone in a room temperature sperm storage medium. Spermatozoa were incubated in eBWW with and without rosiglitazone for 6 days at 22°C. Total motility (**A**) and progressive motility (**B**) were analyzed using CASA every 48 h (n = 9). Data points represent total motility mean values ± SEM at each time point. Asterisk represents significant difference from eBWW control, determined by nonparametric Wilcoxon test ($^{*}P < 0.05$).

initial support to the role of AMPK phosphorylation in the maintenance of sperm function (Fig. 2). Furthermore, rosiglitazone treatment of sperm samples was consistently associated with higher levels of AMPK phosphorylation (Fig. 4, A–C), suggesting that this compound is able to activate AMPK in spermatozoa as in other cell types [23, 25, 48]. A correlation between sperm motility and AMPK phosphorylation in untreated spermatozoa further indicates a role for this kinase in supporting adequate ATP production for sustaining the energy demands of motility (Fig. 4C).

The capacity of AMPK activation to drive a metabolic shift away from mitochondrial OXPHOS substantiates the dramatically reduced mitochondrial ROS seen with rosiglitazone treatment of sperm in this study (Fig. 2D), since mitochondrial electron transport chain leakage is the main source of ROS production in the spermatozoon [6, 49]. This, too, is consistent with the posit that rosiglitazone exerts its effects on

spermatozoa via the AMPK system, and with previous findings, where AMPK activation enhanced the cellular defense against mitochondrial ROS damage and mitochondrial dysfunction in other cell types [50–52].

The improved mMP in rosiglitazone-treated spermatozoa (Fig. 2E) is consistent with the reported protective effects of both rosiglitazone [53] and AMPK activation [50] on mitochondrial integrity. We did not investigate the specific mechanism involved, but presume that mMP is increased secondarily to reduced mitochondrial ROS damage, combined with an overall reduction in mitochondrial involvement in metabolism, due to the rosiglitazone-induced shift away from OXPHOS. Another contributor to maintenance of mMP may be the direct effect of inhibitory phosphorylation of GSK3β downstream of AMPK activation, as seen with resveratrol-induced cytoprotection [52].

To further probe the importance of active AMPK signaling in stallion spermatozoa, we again employed an inhibitor, CC, of this enzyme system. We confirmed that CC decreases sperm AMPK phosphorylation, and concomitantly decreases motility without precipitating a loss in viability (Fig. 5). Thus, consistent with observations in boar sperm [54], it is evident that maintenance of AMPK in an active, phosphorylated state is important for supporting sperm motility.

Previous attempts to activate stallion sperm AMPK with exogenous AMP and pharmacological activators, such as 5-aminoimidazole-4-carboxamide ribonucleotide (AICAR), have been ambiguous [35]. This may be attributed to the mechanism of action of AICAR, which is phosphorylated into 5-amino-4-imidazolecarboxamide ribotide (ZMP)—an analog of AMP that mimics its cellular effects—in combination with the apparent inability of AMP to activate AMPK specifically in sperm cells [55]. Stallion spermatozoa possess 5′nucleotidase [56], an enzyme located at the sperm surface and capable of degrading both AMP [57] and ZMP [58]. It is therefore plausible that such an enzyme facilitates the processing of exogenous AMP and its analogs before they are able to induce substantial phosphorylation of AMPK.

Stallion spermatozoa rely predominantly on OXPHOS for the ATP production that drives motility [2], which, under usual conditions, is a much more efficient means of generating ATP than glycolysis. However, in circumstances where the rate of glucose uptake is very high, a shift to glycolytic catabolism becomes the more efficient option [59]. Notably, in the present study, we saw both an increase in glucose uptake and an increase in ATP content of spermatozoa upon incubation with rosiglitazone (Fig. 2F), seemingly exemplifying the phenomenon described by Vazquez et al. [59], and presumably mediated by AMPK's ability to stimulate glycolysis and increase cellular glucose uptake [60].

Metabolic flexibility, and in particular the ability to switch to glucose utilization, represents an important adaptation to stress resulting from energy depletion, high energy demand, and low oxygen availability. Spermatozoa, both in vivo and in vitro, frequently experience such conditions; motility and capacitation consume large amounts of ATP [61], while minimal cytoplasmic volumes limit the capacity for storing catabolic reserves, and media and biological fluids constitute oxygen-poor environments. In the case of in vitro conditions, oxygen levels are rapidly depleted, and spermatozoa are often immersed in relatively high concentrations of glucose, which is of equivocal benefit to stallion spermatozoa in light of their preference for OXPHOS and relatively poor capacity for glucose utilization [2, 3]. A state of metabolic inflexibility also characterizes the cellular pathophysiology of diabetes (i.e., excess glucose flux to non-insulin-sensitive tissues), and researchers in this field have been working toward development of treatments that restore the ability of cells to select appropriate metabolic substrates and utilize them effectively to produce ATP [15, 62]. The AMPK system has emerged as a key target of such strategies [63–65], given that it can stimulate glucose uptake and processing via multiple downstream signaling pathways, and is central in the cellular response to energetic depletion.

The present study demonstrates that the principle of enhancing metabolic flexibility is applicable to spermatozoa. Rosiglitazone, an AMPK-activating antidiabetic compound, clearly alleviated the deterioration of spermatozoa incubated in conditions of cellular stress. This was exemplified by significant differences in motility, ATP content, mitochondrial superoxide production, mMP, and glucose uptake of spermatozoa exposed to rosiglitazone. A shift to glycolytic metabolism was evidenced by reduced mitochondrial activity (reduced superoxide production and conserved mMP) and increased glucose uptake concurrent with increased ATP production. Furthermore, inclusion of rosiglitazone in a room temperature sperm storage medium supported sperm motility at above 60% for at least 6 days, demonstrating the potential of this compound to improve practical sperm storage outcomes. Whether the beneficial effects of rosiglitazone on sperm quality in vitro will translate into enhanced fertilizing ability in vivo remains to be seen in future trials. Nevertheless, the capacity to manipulate sperm substrate utilization, as demonstrated in this study, unveils exciting new prospects for improving in vitro storage of equine spermatozoa.

REFERENCES

1. Storey BT. Mammalian sperm metabolism: oxygen and sugar, friend and foe. Int J Dev Biol 2008; 52:427–437.
2. Gibb Z, Lambourne SR, Aitken RJ. The paradoxical relationship between stallion fertility and oxidative stress. Biol Reprod 2014; 91:77.
3. Plaza Davila M, Martin Munoz P, Tapia JA, Ortega Ferrusola C, Balao da Silva CC, Pena FJ. Inhibition of mitochondrial complex I leads to decreased motility and membrane integrity related to increased hydrogen peroxide and ATP reduced production, while the inhibition of glycolysis has less impact on sperm motility. PLoS One 2015; 10:e0138777.
4. Tourmente M, Villar-Moya P, Rial E, Roldan ER. Differences in ATP generation via glycolysis and oxidative phosphorylation and relationships with sperm motility in mouse species. J Biol Chem 2015; 290: 20613–20626.
5. Halliwell B, Gutteridge JMC. Free Radicals in Biology and Medicine, 3rd ed. Oxford, UK: Oxford University Press; 2003.
6. Koppers AJ, De Iuliis GN, Finnie JM, McLaughlin EA, Aitken RJ. Significance of mitochondrial reactive oxygen species in the generation of oxidative stress in spermatozoa. J Clin Endocrinol Metab 2008; 93: 3199–3207.
7. Aitken RJ, Gibb Z, Mitchell LA, Lambourne SR, Connaughton HS, De Iuliis GN. Sperm motility is lost in vitro as a consequence of mitochondrial free radical production and the generation of electrophilic aldehydes but can be significantly rescued by the presence of nucleophilic thiols. Biol Reprod 2012; 87:110.
8. Pena FJ, Garcia BM, Samper JC, Aparicio IM, Tapia JA, Ferrusola CO. Dissecting the molecular damage to stallion spermatozoa: the way to improve current cryopreservation protocols? Theriogenology 2011; 76: 1177–1186.
9. Sivitz WI, Yorek MA. Mitochondrial dysfunction in diabetes: from molecular mechanisms to functional significance and therapeutic opportunities. Antioxid Redox Signal 2010; 12:537–577.
10. Campbell DL, Douglas LW, Ramge JC. Cannulation of the equine oviduct and chemical analysis of oviduct fluid. Theriogenology 1979; 12:47–59.
11. Bandyopadhyay GK, Yu JG, Ofrecio J, Olefsky JM. Increased malonyl-CoA levels in muscle from obese and type 2 diabetic subjects lead to decreased fatty acid oxidation and increased lipogenesis; thiazolidinedione treatment reverses these defects. Diabetes 2006; 55:2277–2285.
12. Mensink M, Hesselink MK, Russell AP, Schaart G, Sels JP, Schrauwen P. Improved skeletal muscle oxidative enzyme activity and restoration of PGC-1 alpha and PPAR beta/delta gene expression upon rosiglitazone

treatment in obese patients with type 2 diabetes mellitus. Int J Obes (Lond) 2007; 31:1302–1310.
13. Clark M, Thomaseth K, Dirikolu L, Ferguson DC, Hoenig M. Effects of pioglitazone on insulin sensitivity and serum lipids in obese cats. J Vet Intern Med 2014; 28:166–174.
14. Hallsten K, Virtanen KA, Lonnqvist F, Sipila H, Oksanen A, Viljanen T, Ronnemaa T, Viikari J, Knuuti J, Nuutila P. Rosiglitazone but not metformin enhances insulin- and exercise-stimulated skeletal muscle glucose uptake in patients with newly diagnosed type 2 diabetes. Diabetes 2002; 51:3479–3485.
15. Horakova O, Medrikova D, van Schothorst EM, Bunschoten A, Flachs P, Kus V, Kuda O, Bardova K, Janovska P, Hensler M, Rossmeisl M, Wang-Sattler R, et al. Preservation of metabolic flexibility in skeletal muscle by a combined use of n-3 PUFA and rosiglitazone in dietary obese mice. PLoS One 2012; 7:e43764.
16. Lennon R, Welsh GI, Singh A, Satchell SC, Coward RJ, Tavare JM, Mathieson PW, Saleem MA. Rosiglitazone enhances glucose uptake in glomerular podocytes using the glucose transporter GLUT1. Diabetologia 2009; 52:1944–1952.
17. Spiegelman BM. PPAR-gamma: adipogenic regulator and thiazolidinedione receptor. Diabetes 1998; 47:507–514.
18. Lehmann JM, Moore LB, Smith-Oliver TA, Wilkison WO, Willson TM, Kliewer SA. An antidiabetic thiazolidinedione is a high affinity ligand for peroxisome proliferator-activated receptor gamma (PPAR gamma). J Biol Chem 1995; 270:12953–12956.
19. Desvergne B, Wahli W. Peroxisome proliferator-activated receptors: nuclear control of metabolism. Endocr Rev 1999; 20:649–688.
20. Dello Russo C, Gavrilyuk V, Weinberg G, Almeida A, Bolanos JP, Palmer J, Pelligrino D, Galea E, Feinstein DL. Peroxisome proliferator-activated receptor gamma thiazolidinedione agonists increase glucose metabolism in astrocytes. J Biol Chem 2003; 278:5828–5836.
21. Grunewald S, Paasch U, Glander HJ, Anderegg U. Mature human spermatozoa do not transcribe novel RNA. Andrologia 2005; 37:69–71.
22. Feinstein DL, Spagnolo A, Akar C, Weinberg G, Murphy P, Gavrilyuk V, Dello Russo C. Receptor-independent actions of PPAR thiazolidinedione agonists: is mitochondrial function the key? Biochem Pharmacol 2005; 70: 177–188.
23. Wu J, Wu JJ, Yang LJ, Wei LX, Zou DJ. Rosiglitazone protects against palmitate-induced pancreatic beta-cell death by activation of autophagy via 5′-AMP-activated protein kinase modulation. Endocrine 2013; 44: 87–98.
24. Ceolotto G, Gallo A, Papparella I, Franco L, Murphy E, Iori E, Pagnin E, Fadini GP, Albiero M, Semplicini A, Avogaro A. Rosiglitazone reduces glucose-induced oxidative stress mediated by NAD(P)H oxidase via AMPK-dependent mechanism. Arterioscler Thromb Vasc Biol 2007; 27: 2627–2633.
25. Fryer LG, Parbu-Patel A, Carling D. The anti-diabetic drugs rosiglitazone and metformin stimulate AMP-activated protein kinase through distinct signaling pathways. J Biol Chem 2002; 277:25226–25232.
26. Hardie DG, Carling D. The AMP-activated protein kinase—fuel gauge of the mammalian cell? Eur J Biochem 1997; 246:259–273.
27. Kjobsted R, Treebak JT, Fentz J, Lantier L, Viollet B, Birk JB, Schjerling P, Bjornholm M, Zierath JR, Wojtaszewski JF. Prior AICAR stimulation increases insulin sensitivity in mouse skeletal muscle in an AMPK-dependent manner. Diabetes 2015; 64:2042–2055.
28. Florant GL, Fenn AM, Healy JE, Wilkerson GK, Handa RJ. To eat or not to eat: the effect of AICAR on food intake regulation in yellow-bellied marmots (*Marmota flaviventris*). J Exp Biol 2010; 213:2031–2037.
29. Healy JE, Gearhart CN, Bateman JL, Handa RJ, Florant GL. AMPK and ACC change with fasting and physiological condition in euthermic and hibernating golden-mantled ground squirrels (*Callospermophilus lateralis*). Comp Biochem Physiol A Mol Integr Physiol 2011; 159:322–331.
30. Tosca L, Chabrolle C, Dupont J. AMPK: a link between metabolism and reproduction? [in French].Med Sci (Paris) 2008; 24:297–300.
31. Tartarin P, Guibert E, Toure A, Foretz M, Dupont J, Viollet B, Froment P. Involvement of AMPK in testicular function. In: The Endocrine Society's 94th Annual Meeting and Expo; 2012; Houston, TX. DOI:10.1210/endo-meetings.2012.RE.18.SAT-55.
32. Tartarin P, Guibert E, Toure A, Ouiste C, Leclerc J, Sanz N, Briere S, Dacheux JL, Delaleu B, McNeilly JR, McNeilly AS, Brillard JP, et al. Inactivation of AMPKalpha1 induces asthenozoospermia and alters spermatozoa morphology. Endocrinology 2012; 153:3468–3481.
33. Hurtado de Llera A, Martin-Hidalgo D, Rodriguez-Gil JE, Gil MC, Garcia-Marin LJ, Bragado MJ. AMP-activated kinase, AMPK, is involved in the maintenance of plasma membrane organization in boar spermatozoa. Biochim Biophys Acta 2013; 1828:2143–2151.
34. Nguyen TMD, Alves S, Grasseau I, Métayer-Coustard S, Praud C, Froment P, Blesbois E. Central role of 5′-AMP-activated protein kinase in chicken sperm functions. Biol Reprod 2014; 91:121–115.
35. Cordova A, Strobel P, Vallejo A, Valenzuela P, Ulloa O, Burgos RA, Menarim B, Rodriguez-Gil JE, Ratto M, Ramirez-Reveco A. Use of hypometabolic TRIS extenders and high cooling rate refrigeration for cryopreservation of stallion sperm: presence and sensitivity of 5′ AMP-activated protein kinase (AMPK). Cryobiology 2014; 69:473–481.
36. Aquila S, Bonofiglio D, Gentile M, Middea E, Gabriele S, Belmonte M, Catalano S, Pellegrino M, Ando S. Peroxisome proliferator-activated receptor (PPAR)gamma is expressed by human spermatozoa: its potential role on the sperm physiology. J Cell Physiol 2006; 209:977–986.
37. Seimandi M, Lemaire G, Pillon A, Perrin A, Carlavan I, Voegel JJ, Vignon F, Nicolas JC, Balaguer P. Differential responses of PPARalpha, PPARdelta, and PPARgamma reporter cell lines to selective PPAR synthetic ligands. Anal Biochem 2005; 344:8–15.
38. Zhou G, Myers R, Li Y, Chen Y, Shen X, Fenyk-Melody J, Wu M, Ventre J, Doebber T, Fujii N, Musi N, Hirshman MF, et al. Role of AMP-activated protein kinase in mechanism of metformin action. J Clin Invest 2001; 108:1167–1174.
39. Gibb Z, Lambourne SR, Quadrelli J, Smith ND, Aitken RJ. L-carnitine and pyruvate are prosurvival factors during the storage of stallion spermatozoa at room temperature. Biol Reprod 2015; 93:104.
40. Whitten WK, Biggers JD. Complete development in vitro of the pre-implantation stages of the mouse in a simple chemically defined medium. J Reprod Fertil 1968; 17:399–401.
41. Blanchard TL, Varner DD, Love CC, Hurtgen JP, Cummings MR, Kenney RM. Use of a semen extender containing antibiotic to improve the fertility of a stallion with seminal vesiculitis due to *Pseudomonas aeruginosa*. Theriogenology 1987; 28:541–546.
42. Aitken RJ, Smith TB, Lord T, Kuczera L, Koppers AJ, Naumovski N, Connaughton H, Baker MA, De Iuliis GN. On methods for the detection of reactive oxygen species generation by human spermatozoa: analysis of the cellular responses to catechol oestrogen, lipid aldehyde, menadione and arachidonic acid. Andrology 2013; 1:192–205.
43. Riek U, Scholz R, Konarev P, Rufer A, Suter M, Nazabal A, Ringler P, Chami M, Muller SA, Neumann D, Forstner M, Hennig M, et al. Structural properties of AMP-activated protein kinase: dimerization, molecular shape, and changes upon ligand binding. J Biol Chem 2008; 283:18331–18343.
44. Swegen A, Aitken RJ. Characterisation of the stallion sperm proteome. J Equine Vet Sci 2014; 34:35–37.
45. Schaefer KL, Takahashi H, Morales VM, Harris G, Barton S, Osawa E, Nakajima A, Saubermann LJ. PPARgamma inhibitors reduce tubulin protein levels by a PPARgamma, PPARdelta and proteasome-independent mechanism, resulting in cell cycle arrest, apoptosis and reduced metastasis of colorectal carcinoma cells. Int J Cancer 2007; 120:702–713.
46. Bhagwat S, Dalvi V, Chandrasekhar D, Matthew T, Acharya K, Gajbhiye R, Kulkarni V, Sonawane S, Ghosalkar M, Parte P. Acetylated alpha-tubulin is reduced in individuals with poor sperm motility. Fertil Steril 2014; 101:95–104.e103.
47. Hurtado de Llera A, Martin-Hidalgo D, Gil MC, Garcia-Marin LJ, Bragado MJ. AMP-activated kinase AMPK is expressed in boar spermatozoa and regulates motility. PLoS One 2012; 7:e38840.
48. Yang S, Luo T, Zhou H, Lv Q, Liu L, Zhang W, Gao R, Chen S, Xia W, Luo M, Cheng Q, Li Q. Rosiglitazone inhibits expression and secretion of PEDF in adipose tissue and liver of male SD rats via a PPAR-gamma independent mechanism. Endocrinology 2014; 155:941–950.
49. Holland MK, Storey BT. Oxygen metabolism of mammalian spermatozoa: generation of hydrogen peroxide by rabbit epididymal spermatozoa. Biochem J 1981; 198:273–280.
50. Dong GZ, Lee JH, Ki SH, Yang JH, Cho IJ, Kang SH, Zhao RJ, Kim SC, Kim YW. AMPK activation by isorhamnetin protects hepatocytes against oxidative stress and mitochondrial dysfunction. Eur J Pharmacol 2014; 740:634–640.
51. Wang XR, Zhang MW, Chen DD, Zhang Y, Chen AF. AMP-activated protein kinase rescues the angiogenic functions of endothelial progenitor cells via manganese superoxide dismutase induction in type 1 diabetes. Am J Physiol Endocrinol Metab 2011; 300:E1135–E1145.
52. Shin SM, Cho IJ, Kim SG. Resveratrol protects mitochondria against oxidative stress through AMP-activated protein kinase-mediated glycogen synthase kinase-3beta inhibition downstream of poly(ADP-ribose)polymerase-LKB1 pathway. Mol Pharmacol 2009; 76:884–895.
53. Quintanilla RA, Jin YN, Fuenzalida K, Bronfman M, Johnson GV. Rosiglitazone treatment prevents mitochondrial dysfunction in mutant huntingtin-expressing cells: possible role of peroxisome proliferator-activated receptor-gamma (PPARgamma) in the pathogenesis of Huntington disease. J Biol Chem 2008; 283:25628–25637.

54. Martin-Hidalgo D, Hurtado de Llera A, Yeste M, Cruz Gil M, Bragado MJ, Garcia-Marin LJ. Adenosine monophosphate-activated kinase, AMPK, is involved in the maintenance of the quality of extended boar semen during long-term storage. Theriogenology 2013; 80:285–294.
55. Vadnais ML, Cao W, Aghajanian HK, Haig-Ladewig L, Lin AM, Al-Alao O, Gerton GL. Adenine nucleotide metabolism and a role for AMP in modulating flagellar waveforms in mouse sperm. Biol Reprod 2014; 90: 128.
56. Swegen A, Curry BJ, Gibb Z, Lambourne SR, Smith ND, Aitken RJ. Investigation of the stallion sperm proteome by mass spectrometry. Reproduction 2015; 149:235–244.
57. Minelli A, Liguori L, Bellezza I, Renieri T, Castellini C. Effects of diadenosine polyphosphates and seminal fluid vesicles on rabbit sperm cells. Reproduction 2003; 125:827–835.
58. Pesi R, Micheli V, Jacomelli G, Peruzzi L, Camici M, Garcia-Gil M, Allegrini S, Tozzi MG. Cytosolic 5′-nucleotidase hyperactivity in erythrocytes of Lesch-Nyhan syndrome patients. Neuroreport 2000; 11: 1827–1831.
59. Vazquez A, Liu J, Zhou Y, Oltvai ZN. Catabolic efficiency of aerobic glycolysis: the Warburg effect revisited. BMC Syst Biol 2010; 4:58.
60. Kwon Y, Song P, Yoon JH, Ghim J, Kim D, Kang B, Lee TG, Kim JA, Choi JK, Youn IK, Lee HK, Ryu SH. Xanthene derivatives increase glucose utilization through activation of LKB1-dependent AMP-activated protein kinase. PLoS One 2014; 9:e108771.
61. Ferramosca A, Zara V. Bioenergetics of mammalian sperm capacitation. Biomed Res Int 2014; 2014:902953.
62. Stephenson EJ, Smiles W, Hawley JA. The relationship between exercise, nutrition and type 2 diabetes. Med Sport Sci 2014; 60:1–10.
63. Qi D, Young LH. AMPK: energy sensor and survival mechanism in the ischemic heart. Trends Endocrinol Metab 2015; 26:422–429.
64. Ramesh M, Vepuri SB, Oosthuizen F, Soliman ME. Adenosine monophosphate-activated protein kinase (AMPK) as a diverse therapeutic target: a computational perspective. Appl Biochem Biotechnol 2016; 178: 810–830.
65. Gasparrini M, Giampieri F, Alvarez Suarez JM, Mazzoni L, Forbes Hernandez TY, Quiles JL, Bullon P, Battino M. AMPK as a new attractive therapeutic target for disease prevention: the role of dietary compounds. Curr Drug Targets 2016; 17:865–889.